Article

Cytotoxicity of Biogenic Gold Nanoparticles against Lung Cancer Cell Line (A549): An Application Oriented Perspective

Babita Jha[1], Kamal Prasad[2,*] and Anal K. Jha[1,*]

[1] Aryabhatta Centre for Nanoscience and Nanotechnology, Aryabhatta Knowledge University, Patna 800001, India; babita.jha20@gmail.com (B.J.); analkjha80@gmail.com (A.K.J.)
[2] University Department of Physics, T.M. Bhagalpur University, Bhagalpur 812007, India; prasad_k@tmbuniv.ac.in
* Correspondence: prasad_k@tmbuniv.ac.in (K.P.); analkjha80@gmail.com (A.K.J.)

Abstract: The present work encompasses an application-oriented perspective to the possible employment of gold nanoparticles as nanomedicine in cancer therapeutics. The rationale of the work lies in the growing needs for assessment of advanced alternative treatment of cancer employing functionalized nanoparticles as nanomedicine. Gold nanoparticles fabricated *via* green chemistry methods by leaves of a time-honored medicinal plant, *Piper betle* were ascertained for their synthesis and properties under the umbrella of characterization of nanoparticles, through various techniques like UV-vis spectroscopy, FTIR spectroscopy, X-ray diffraction, and scanning electron microscopy. The cytotoxicity assay of well-characterized gold nanoparticles was monitored against lung cancer cell line (A549) by metabolic and imaging assays. MTT assay or the metabolic assay was performed for a range of nanoparticles' concentrations. The results were promising and proved to be a leading-edge venture, envisaging the possibility of gold nanoparticles for cancer therapeutics.

Keywords: Gold nanoparticles; Green chemistry; *Piper betle;* Lung cancer cell line (A549); Nanomedicine

1. Introduction

Nanotechnology has emerged as a disruptive technology leading to discontinuous innovations with the ability to radically change the existing scenario for the substantial improvement of human civilization. The conversion of these probabilities to possibility requires a considerable level of mature efforts with rationale objective in fabrication and application of the bunch of nano-entities. The pharmacological significance of the nanoparticles has opened new avenues for their applicability in the cure of many deadly diseases, cancer being one of them. Nanoscience and nanotechnology have enrolled in all the domains of cancer research *i.e.* diagnostics, monitoring and therapeutics providing novel services in these areas [1]. Among the plethora of nanoparticles utilized for cancer research, the gold nanoparticles have significant importance owing to their high stability, sensitivity and high level of consistency [2]. The gold nanoparticles are known for their potent anti-proliferative effects against various carcinoma [3]. With the increasing implementation of gold nanoparticles in biomedical applications there is an urge for biological and environmental safety in their production. The rationale of the present research work lies in the growing needs for assessment of advanced alternative treatment of cancer employing biocompatible functionalized gold nanoparticles as nanomedicine. This work encompasses the genesis of gold nanoparticles (abbreviated hereafter as AuNPs) by a simple, reliable, energy efficient, bio-compatible, cost-effective and eco-friendly fabrication route employing leaves of a time-honored medicinal plant, *Piper betle* via green chemistry methods. The plant is rich in phytoconstituents with the major

 doi:10.20944/preprints201812.0308.v1

share of polyphenols having strong antioxidant properties making them a good bioreductant and stabilizer [4,5]. There are reports wherein these plants have been efficiently used to fabricate other metallic nanoparticles like silver nanoparticles [6]. The phytochemicals besides evoking nanotransformation, binds up with the fabricated nanoparticles as capping agents adding on to its therapeutic efficacy [7]. The fabricated functionalized AuNPs were characterized by using techniques like UV-vis. and FTIR spectroscopy along with structural analysis using X-ray diffraction, and surface imaging by scanning electron microscopy studies. The cytotoxicity assay of well-characterized gold nanoparticles was monitored against lung cancer cell line (A549) by metabolic and imaging assays to look forth for their possible application as an antitumor agent. The present work hopes to look forward to perspectives of revolutionizing cancer therapeutics through alternate nanomedicine.

2. Materials and Methods

2.1. Preparation of AuNPs

Fresh and healthy *Piper betle* leaves were thoroughly washed in running tap water and rinsed with distilled water then after surface sterilized with ethanol. The ethanol swabbed plant parts were then washed with sterile water and finally air dried. 10 gm of the air-dried leaves were finely chopped and placed in a beaker with 100 ml of 50% ethanol and boiled on a steam bath for 15 minutes until the colour of the solution turned to dark green. On cooling, the solution was double filtered to be used as source extract aiding in nanotransformation. Analytical grade Gold (III) chloride trihydrate salt procured from Hi-media Lab Pvt. Ltd., Mumbai, India was used, and 0.025 M salt solution was prepared in distilled water. 10ml of ethanolic *Piper betle* leaves extract was diluted with 90 ml of distilled water in a conical flask and placed in boiling water bath. To this 10 ml of aqueous Gold (III) chloride salt solution (0.025 M) was added maintaining the basic pH conditions through analytical grade aqueous Sodium hydrogen carbonate (Hi-media Lab Pvt. Ltd., Mumbai) salt solution. The nanotransformation reaction was allowed at the basic pH to obtain AuNPs. The fabricated metallic nanoparticles were separated from the colloidal solution by centrifugation at 10,000 rpm for 20 minutes. The clear supernatant was discarded, and the pellet was washed two times with distilled water. The moisture content was removed, and characterization methods pursued.

2.2. Characterization Methods

The absorbance spectrum of the nanoparticle solution after the synthesis was recorded by UV-vis. spectroscopy. This served as the preliminary characterization of the AuNPs. The degree of precursor metal ions conversion to their respective nanoparticles was assessed by UV-vis. spectrum. The spectrum was recorded using a Perkin Elmer spectrophotometer, UK operated at an interval of 1nm coupled with a scan speed of 266.75 nm/min. The Fourier transformed infrared (FTIR) spectrum of the dried powdered sample of AuNPs was collected using Perkin Elmer, UK, FTIR spectrophotometer by KBr pellet method. The data were collected in transmission mode in between the wavelength range of 4500-400 cm^{-1}. The crystal structure and the average particulate size of the powdered sample of AuNPs was studied by X-Ray diffraction. XRD patterns of all the metallic nanoparticles were recorded by Bruker D8-Advance diffractometer with Cu-Kα radiation source. The microstructural study of the dried powdered sample of AuNPs was carried out by a scanning electron microscope (SEM). The SEM micrograph was taken by EVO 18, Carl Zeiss Microscopy Ltd., UK after coating with a thin layer of gold-palladium sputter coater after mounting on stubs.

2.3. Cytotoxicity Assay

The cytotoxicity assay of AuNPs was assessed against lung cancer cell line (A549) obtained from NCCS, Pune, India. The cell line was cultured in the growth media Rosewell Park Memorial Institute 1640 (RPMI 1640) with 10% fetal bovine serum (FBS) and 1% antibiotic (pen-strep) obtained from Hi-Media, Mumbai, India, maintaining the physiological pH and temperature at 37°C and 5%

 doi:10.20944/preprints201812.0308.v1

CO_2. The cytotoxicity effect of AuNPs was assessed by the metabolic assay or the MTT assay. The procedure adapted included the seeding by 100 µl of uniform cell suspension with an appropriate number of cells (as calculated by haemocytometer) in each well of a 96-well plate. The plate was incubated for 24 hrs. The next day the media was aspirated and 100 µl drug mixed media of variable concentrations to be tested were added to each well. Media without drug was added into the control well. After a treatment period of 24 hrs., the media was aspirated and 100 µl of 3-[4, 5-Dimethylthiazol-2-yl]-2, 5-diphenyl tetrazolium bromide (MTT) procured from Hi-Media, Mumbai at the concentration of 5 mg/ml in 1X PBS was added to each well. The plate was incubated in a CO_2 incubator at 37°C for 4 hrs. The MTT solution was then removed and formazon crystals were dissolved by adding 100 µl of DMSO per well. After 10 minutes incubation in dark conditions, the readings were taken by spectrophotometer at 570 nm. The assay was performed for a range of nanoparticles' concentrations of 5, 10, 25, 50, 75, 100, 150, and 200 µg/ml for the treatment time of 24 hrs. in triplicates. The cell viability is reproduced as percent cell viability considering the viability of untreated cells as 100%. Label-free monitoring of the effect of these nanoparticles on lung cancer cells was pursued by imaging assay using a phase contrast inverted microscope and the image at the highest dose of nanoparticles in the experiment was captured. Statistical significance of the data was observed through the t-test. The results were communicated as mean ± standard errors with *p*-values less than 0.05 considered significant.

3. Results and Discussion

3.1. Nanotransformation to AuNPs

As the reaction proceeded nanotransformation of gold ions to gold nanoparticles by the reducing agents present in plant extract was observed through distinct colour change. Completion of the reaction was observed in the time duration of 25-30 minutes with the final colour of solution being converted to ruby red. Figure 1 illustrates the nanotransformation process aided by the metabolite rich leaves of *Piper betle* to produce the resultant ruby red AuNPs. The colour owes to the surface plasmon vibrations of the gold nanoparticles [8]. The reduction of metallic ion released from the gold salt is due to electron donation to precursor ions by the reducing agents found in the plant extract. The main role of reducing agent precisely is to provide an electron to metal ions to form an elemental atom. The ethanolic extract of medicinal *Piper betle* leaves is known to be rich in phytochemicals and has abundance of alkaloid, steroids, terpenoids, and flavonoids that aid in nanotransformation [9,10]. These phytochemicals also provide an added advantage of stabilizing the nanoparticles by working as capping agents [11].

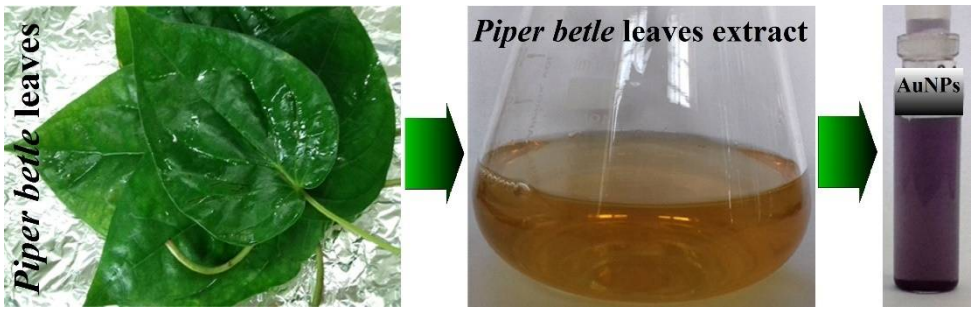

Figure 1. The fabrication of gold nanoparticles by *Piper betle* leaves.(**a**) *Piper betle* leaves; (**b**) the leaves ethanolic extract; (c) the fabricated gold nanoparticles.

3.2. Structure and Microstructureof AuNPs

Prior to the applicability of the gold nanoparticles, it is paramount to be monitored for its fabrication and properties which was done under the umbrella of characterization techniques. The X-ray diffraction profile of AuNPs elucidates the crystalline nature of the particles. As shown in Figure 2(a) four peaks were indexed in the XRD diffraction pattern *i.e.* (111), (200), (220) and (311)

Preprints (www.preprints.org) | NOT PEER-REVIEWED | Posted: 25 December 2018 doi:10.20944/preprints201812.0308.v1

which were assigned to the planes of face-centered cubic (fcc) structure. The length of unit cell edge was estimated to be 4.0782Å which agrees with standard literature (ICDD no. #65-2870). The apparent crystallite size was estimated using the Debye-Scherrer formula: $P_{hkl} = 0.89\lambda/B\cos\theta$; where B = full width at half maximum and was found to be ~10 nm. As the crystallites are very smaller, the parallel planes available for sharp diffraction are meagerly resulting in broadening of peaks affirming the nanosize of fabricated AuNPs. The small crystallite size of the AuNPs probably aids in cellular uptake of these nanoparticles through diffusion and endocytosis. Figure 2(b) depicts the SEM image of the fabricated AuNPs. It revealed the surface topography that was observed to be nearly spherical in structure and the formations of nanosized particles some of which clubbed together due to high surface energy.

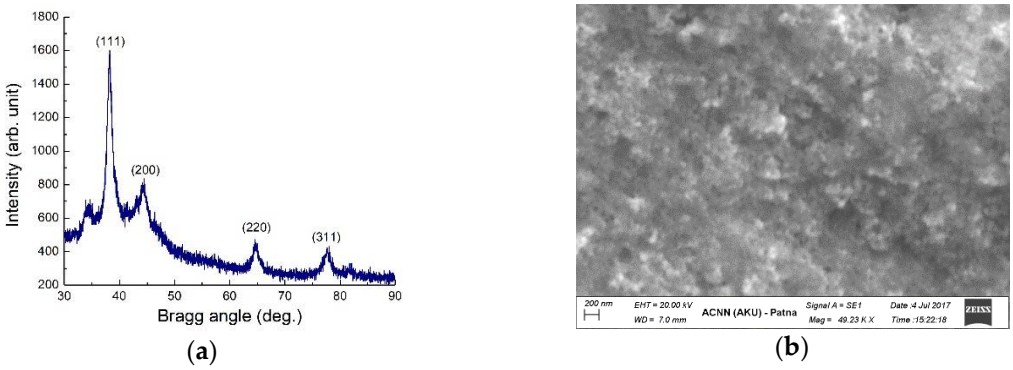

(**a**) (**b**)

Figure 2. (**a**) X-ray diffraction pattern; (**b**) SEM micrograph of AuNPs at room temperature.

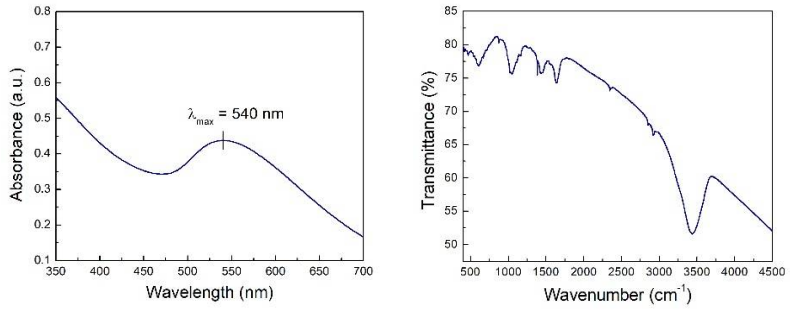

(**a**) (**b**)

Figure 3. (**a**) UV-vis absorbance spectrum; (**b**) FT-IR spectrum of AuNPs at room temperature.

3.3. UV-vis. and FTIR Spectraof AuNPs

The UV-vis. spectroscopy study is an important tool to comprehend the final formation of nanoparticles. Figure 3(a) displays the UV–vis. spectrum recorded from aqueous *Piper betle* leaves extract–$HAuCl_4$ (0.025M) solution. The generation of colour (Figure 1) is due to excitation of surface plasmons in AuNPs and interaction with candidate metabolites. The surface plasmon band of AuNPs centralized at 540nm in the visible range which ascertained the characteristic absorbance of gold nanoparticles [12]. Also, the broadened plasmon band could be due to the size distribution of the particles. The FTIR spectrum or the vibrational spectrum arising due to vibrational motion of the molecules present on the AuNPs upon interaction with IR radiation is a unique characteristic physical property. The basic interpretation of the spectrum brings about information about the structural features and functional groups attached to the molecules that are characteristic and identifiable [13]. The intensity of the peaks is primarily attributed to the stretching vibrations due to diverse functional groups. Figure 3(b) reveals the FTIR spectra of fabricated AuNPs. The absorption peak at 3704 cm^{-1} is attributed to O-H stretching vibration and the peak at 3436 cm^{-1} is due to intramolecular H-bond. The amide (I/II) region comprises of the region between 1700 cm^{-1} to 1500 cm^{-1} [14] wherein peaks at 1766 cm^{-1}, 1638 cm^{-1} and 1529 cm^{-1} are due to C=O , C=C and C=N

Preprints (www.preprints.org) | NOT PEER-REVIEWED | Posted: 25 December 2018 doi:10.20944/preprints201812.0308.v1

stretching vibrations respectively. The peak at 1431 cm^{-1} is due to C-H and C-H_2 deformation vibration. The peaks at 1393 cm^{-1}, 1384 cm^{-1}, and 1225 cm^{-1} are because of CH_3 symmetrical bending, O-H deformation, C-O stretching vibration, C-H skeletal and deformation vibrations. The fingerprint region had multiple peaks owing to diversiform vibration acting as a characteristic feature. The data communicates of the possible interactions between the *Piper betle* phytochemicals and the AuNPs that aids in the fabrication and functionalization of the nanoparticles.

3.4. CytotoxicPotentialAssay of AuNPs

The biogenic gold nanoparticles were assessed for their cytotoxic activity against lung cancer cell line (A549) by incubating them with varying concentrations of the AuNPs for 24 hrs. The metabolic assay, MTT assay was adopted for determination of cell viability. It was observed that AuNPs cut off the growth of cancer cells significantly (***$p < 0.001$) with inhibition of 49.46% of cells as compared to the control, at the dose of 200 µg/ml. The results shown in Figure 4 indicate that different concentrations of AuNPs have varied cytotoxic effects on A549 cell line. The cell viability as compared to control at 5 µg/ml was 98.46% (difference not significant $p > 0.05$); for 10 µg/ml was 96.70% (difference not significant $p > 0.05$); for 25 µg/ml was 90.35% (*$p < 0.05$); for 50 µg/ml was 87.10% (**$p < 0.01$); for 75 µg/ml was 82.53% (***$p < 0.001$); for 100 µg/ml was 59.08% (***$p < 0.001$); for 150 µg/ml was 57.34% (***$p < 0.001$) and for 200 µg/ml was 50.53% (***$p < 0.001$). The cytotoxicity was observed with the maximal effect obtained at the concentration of 200 µg/ml of the tested range of dose of AuNPs. A noticeable effect of the cytotoxicity of AuNPs on cultured cells was apparent with the alterations in the morphology of the monolayer culture. As shown in Figure 5 the (untreated) control cells appeared to be closely aligned; whereas, the AuNPs treated cells contracted, lost adherence and floated in the media symbolizing the significant effect of nanoparticles on cells [15]. The cellular uptake of the AuNPs leads to toxicity probably due to physiochemical interaction of gold atoms with the intracellular proteins and DNA [16], ending up in cell death. The cell viability was found to decrease with the increasing concentration of AuNPs that added up to the fact that more the physiochemical interaction of gold ions the greater the cytotoxicity up to a threshold level. Besides the concentration of nanoparticles, particle size and the time of exposure are important variables for desirable results. The accumulation of smaller nanoparticles at tumor sites are massed owing to their elopement by the reticuloendothelial system capture [17]. AuNPs are advantageous over other metal nanoparticles by virtue of their biocompatibility and non-cytotoxicity [18]. In the present context, the AuNPs fabricated and stabilized through metabolically rich plant source are encircled with therapeutically significant phytoconstituents that aids on to its biocompatibility and therapeutic efficacy.

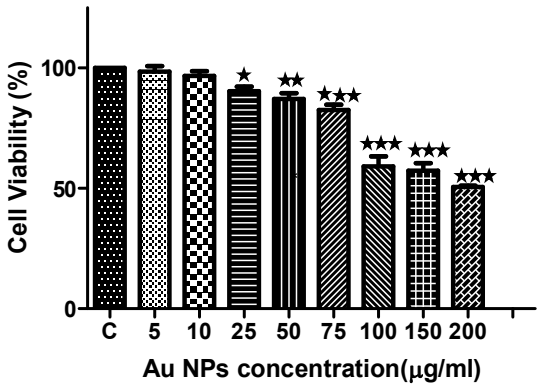

Figure 4. Effect of different concentrations of AuNPs on cell viability of A549 cancer cell lines. Data presented as mean ± SE of experiment done in triplicates. *$p < 0.05$, **$p < 0.01$, ***$p < 0.001$ versus the control.

 doi:10.20944/preprints201812.0308.v1

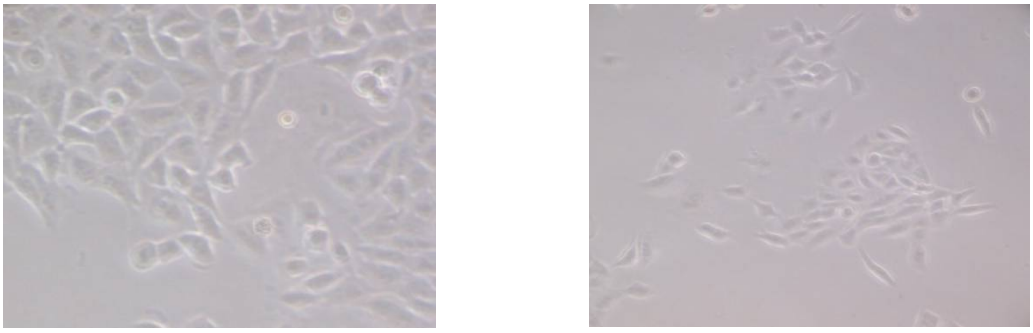

(**a**) (**b**)

Figure 5. Microscopic photographs of AuNPs treated A549 lung cancer cell line: (**a**) The untreated cells; (**b**) Cells treated with 200µg/ml of AuNPs.

4. Conclusions

Experiments at the cellular level are the bottleneck for elucidating the therapeutic potency of drugs. Herein, in vitro cytotoxic effect of biologically fabricated and functionalized AuNPs against A549, an epithelial cell line derived from human lung cancer has been witnessed. AuNPs of ~10 nm crystallite size significantly inhibited the proliferation of lung carcinoma cells. The major drawback with the prevailing chemotherapeutic drugs lies in their systemic toxicity and drug resistance [19] therefore AuNPs emerges out as a biocompatible option that besides improving the bioavailability works as an effective therapeutic drug with minimal side effects. Overall, these findings have forecasted that biologically fabricated and functionalized AuNPs obtained from *Piper betle* could be potential lung carcinoma drug. The fabrication of biocompatible functionalized nanoparticles could also be scaled up through tissue culture techniques [20]. Further studies elucidating the molecular mechanistic aspect of its action and genotoxicity studies through *in-vivo* models is of paramount need, but the present results are promising and prove to be a leading-edge venture, envisaging the possibility of gold nanoparticles for cancer therapeutics.

Author Contributions: All authors contributed to the conceptualization, methodology, formal analysis, writing, editing and proof reading of the manuscript. All the investigations were carried out by B.J. The final version of the manuscript was approved by all authors.

Funding: This research received no external funding.

Conflicts of Interest: The authors declare no conflict of interest.

References

1. Maeng, J. H.; Lee, D.-H.; Jung, K. H.; Bae, Y.-H.; Park, I.-S.; Jeong, S.; Jeon, Y.-S.; Shim, C.-K.; Kim, W.; Kim, J.; et al. Multifunctional Doxorubicin Loaded Superparamagnetic Iron Oxide Nanoparticles for Chemotherapy and Magnetic Resonance Imaging in Liver Cancer. *Biomaterials* **2010**, *31*(18), 4995–5006. https://doi.org/10.1016/j.biomaterials.2010.02.068.
2. Huang, X.; Jain, P. K.; El-Sayed, I. H.; El-Sayed, M. A. Determination of the Minimum Temperature Required for Selective Photothermal Destruction of Cancer Cells with the Use of Immunotargeted Gold Nanoparticles. *Photochemistry and Photobiology* **2006**, *82*(2), 412–417. https://doi.org/10.1562/2005-12-14-RA-754.
3. Daduang, J.; Palasap, A.; Daduang, S.; Boonsiri, P.; Suwannalert, P.; Limpaiboon, T. Gallic Acid Enhancement of Gold Nanoparticle Anticancer Activity in Cervical Cancer Cells. *Asian Pacific Journal of Cancer Prevention* **2015**, *16*(1), 169–174. https://doi.org/10.7314/APJCP.2015.16.1.169.
4. Chauhan, E. S.; Aishwarya, J.; Singh, A.; Tiwari, A. A Review: Nutraceuticals Properties of *Piper Betel* (Paan). *American Journal of Phytomedicine and Clinical Therapeutics* **2016**, *4*(02), 028–041.
5. Pradhan, D.; Suri, D. K. A.; Pradhan, D. D. K.; Biswasroy, P. Golden Heart of the Nature *Piper Betle* L. *Journal of Pharmacognosy and Phytochemistry* **2013**, *1*(6), 147–167.

6. Jha, B.; Rao, M.; Prasad, K.; Jha, A. K. Evaluation of Antimicrobial Activity of Silver Nanoparticles Synthesized from *Piper Betle* Leaves against Human and Plant Pathogens.*AIP Conference Proceedings* **2018**,*1953*, 030257–4. https://doi.org/10.1063/1.5032592.
7. Iravani, S. Green Synthesis of Metal Nanoparticles Using Plants. *Green Chemistry* **2011**, *13*(10), 2638–2650. https://doi.org/10.1039/c1gc15386b.
8. Rajasekharreddy, P.; Usha Rani, P.; Sreedhar, B. Qualitative Assessment of Silver and Gold Nanoparticle Synthesis in Various Plants: A Photobiological Approach. *Journal of Nanoparticle Research* **2010**, *12*(5), 1711–1721. https://doi.org/10.1007/s11051-010-9894-5.
9. Dauthal, P.; Mukhopadhyay, M. Noble Metal Nanoparticles: Plant-Mediated Synthesis, Mechanistic Aspects of Synthesis, and Applications. *Industrial & Engineering Chemistry Research* **2016**, *55*(36), 9557–9577. https://doi.org/10.1021/acs.iecr.6b00861.
10. Durán, N.; Marcato, P. D.; Durán, M.; Yadav, A.; Gade, A.; Rai, M. Mechanistic Aspects in the Biogenic Synthesis of Extracellular Metal Nanoparticles by Peptides, Bacteria, Fungi, and Plants. *Applied Microbiology and Biotechnology* **2011**, *90*(5), 1609–1624. https://doi.org/10.1007/s00253-011-3249-8.
11. Akhtar, M. S.; Panwar, J.; Yun, Y.-S. Biogenic Synthesis of Metallic Nanoparticles by Plant Extracts. *ACS Sustainable Chemistry & Engineering* **2013**, *1*(6), 591–602. https://doi.org/10.1021/sc300118u.
12. Govindaraju, K.; Basha, S. K.; Kumar, V. G.; Singaravelu, G. Silver, Gold and Bimetallic Nanoparticles Production Using Single-Cell Protein (Spirulina Platensis) Geitler. *Journal of Materials Science* **2008**, *43*(15), 5115–5122. https://doi.org/10.1007/s10853-008-2745-4.
13. Coates, J. Interpretation of Infrared Spectra, A Practical Approach. In *Encyclopedia of Analytical Chemistry*; Meyers, R. A., Ed.; John Wiley & Sons, Ltd: Chichester, UK, **2006**. https://doi.org/10.1002/9780470027318.a5606.
14. Baker, M. J.; Trevisan, J.; Bassan, P.; Bhargava, R.; Butler, H. J.; Dorling, K. M.; Fielden, P. R.; Fogarty, S. W.; Fullwood, N. J.; Heys, K. A.; et al. Using Fourier Transform IR Spectroscopy to Analyze Biological Materials. *Nature Protocols* **2014**, *9*(8), 1771–1791. https://doi.org/10.1038/nprot.2014.110.
15. Mishra, A.; Mehdi, S. J.; Irshad, M.; Ali, A.; Sardar, M.; Moshahid, M.; Rizvi, A. Effect of Biologically Synthesized Silver Nanoparticles on Human Cancer Cells. *Science of Advanced Materials* **2012**, *4*(12), 1200–1206. https://doi.org/10.1166/sam.2012.1414.
16. Hackl, E. V.; Blagoi, Y. P. Effect of Ethanol on Structural Transitions of DNA and Polyphosphates under Ca^{2+} Ions Action in Mixed Solutions.*Acta BiochimicaPolonica* **2000**, *47*(1), 103–112.
17. Sutradhar, K. B.; Amin, M. L. Nanotechnology in Cancer Drug Delivery and Selective Targeting. *ISRN Nanotechnology* **2014**, *2014*, 1–12. https://doi.org/10.1155/2014/939378.
18. Kamala Priya, M. R.; Iyer, P. R. Anticancer Studies of the Synthesized Gold Nanoparticles against MCF 7 Breast Cancer Cell Lines. *Applied Nanoscience* **2015**, *5*(4), 443–448. https://doi.org/10.1007/s13204-014-0336-z.
19. Kelloff, G. J. Perspectives on Cancer Chemoprevention Research and Drug Development. In *Advances in Cancer Research* **1999**, 78, 199–334. https://doi.org/10.1016/S0065-230X(08)61026-X.
20. Jha, A. K.; Prasad, K.; Prasad, K.; Kulkarni, A. R. Plant System: Nature's Nanofactory. *Colloids and Surfaces B: Biointerfaces* **2009**, *73*(2), 219–223. https://doi.org/10.1016/j.colsurfb.2009.05.018.